

Using imaginary-time time-dependent density functional theory for robust convergence of ground states

Cedric Flamant⁽¹⁾, Grigory Kolesov⁽²⁾, Efstratios Manousakis^(3,4), and Efthimios Kaxiras^(1,2)

⁽¹⁾*Department of Physics, Harvard University,
Cambridge, Massachusetts 02138, USA*

⁽²⁾*John A. Paulson School of Engineering and Applied Sciences,
Harvard University, Cambridge, Massachusetts 02138, USA*

⁽³⁾*Department of Physics and National High Magnetic Field Laboratory,
Florida State University, Tallahassee, Florida 32306-4350, USA*

⁽⁴⁾*Department of Physics, University of Athens,
Panepistimioupolis, Zografos, 157 84 Athens, Greece*

(Dated: May 18, 2022)

Abstract

We transform the time-dependent density functional theory equations to imaginary time and use imaginary-time evolution as a reliable alternative to the self-consistent field (SCF) procedure for determining the Kohn-Sham (KS) ground state. We discuss the technical and theoretical aspects of this approach and show that the ground state of the Kohn-Sham system should be expected to be the long-imaginary-time output of the evolution, independent of chosen functional or level of theory used to simulate the system. By maintaining self-consistency between the single-particle wavefunctions and electronic density throughout the determination of the stationary state, our method avoids some of the difficulties encountered in SCF such as charge sloshing and other unproductive occupancy rearrangements. To demonstrate dependability, we successfully apply our method to selected systems which struggle to converge when standard SCF is employed. Given its minimal required inputs and robust convergence, our method should be a useful tool in applications of density functional theory. Additionally, through the van Leeuwen theorem we affirm the physical meaningfulness of imaginary time in density functional theory, justifying the use of DFT in quantum statistical mechanics such as in computing imaginary time path integrals.

I. INTRODUCTION

Density functional theory (DFT) is a widely successful approach enabling *ab initio* calculations of electronic and material properties. Unlike direct approaches to studying quantum systems through the Schrödinger equation where the wavefunction is the central mathematical object, density functional theory uses the electron density distribution as the fundamental field. In principle, through the Hohenberg-Kohn theorem¹, the ground state electron density of a system uniquely determines all of its observables. It is standard practice to use the Kohn-Sham (KS) system² of non-interacting fermions as a shortcut to obtaining the ground state density, employing specially formulated potentials^{3,4} that are functionals of the density to approximate the electron-electron interactions.

There are many techniques to find the ground state of the KS equations, which include methods which (a) aim at direct determination of the minimum of the KS total energy functional⁵⁻⁷, and (b), use more traditional iterative methods based on diagonalization of the KS Hamiltonian in conjunction with iterative improvements of the ground state charge density through mixing. The work presented in this paper is distinct from both these categories, and we focus on comparing our method to the approaches of type (b). For a system with N electrons, the lowest N eigenstates to the KS equations determine the electronic density, which itself appears in the KS equations through an effective single-particle potential. Thus, the equations have to be solved self-consistently to represent a physical configuration. In general, finding the set of N eigenstates that satisfy the KS equations involves an iterative process known as self-consistent field (SCF) iterations which produce successively better approximations to the equations' solution. In its simplest conceptualization the iterative approach involves solving the eigenvalue problem for an initial density distribution, then using the resulting eigenstates to produce the next approximation to the density. When this approach is iterated, except for the simplest systems it rarely converges to a self-consistent solution. In order to stabilize the SCF loops and improve the convergence rate, various mixing schemes are employed in DFT calculations. These schemes take advantage of the information contained in multiple previous trial densities to better select the next one. A popular mixing scheme is Pulay mixing^{8,9}, also known as direct inversion of the iterative subspace (DIIS).

While SCF loops work well for a wide variety of systems, occasionally one encounters

systems which require many iterations to reach an acceptable solution, or worse yet, those where SCF loops do not make any progress. In such situations one can try changing the mixing scheme or its parameters, starting with a different density, or fractionally occupying states^{10,11} which some methods implement by introducing a fictitious electronic temperature (Fermi smearing^{12,13}). These approaches can sometimes coax the process to convergence. If not, one can resort to computationally-intensive direct minimization methods⁵⁻⁷ to find a solution. The convergence difficulties for SCF usually arise in systems with large unit cells and in metallic systems¹⁴, or when an excited state is desired. The small differences in eigenenergies of the single-particle states, as well as the presence of many states near the Fermi level or the highest occupied state in the case of excited systems, can cause very different eigenstates to be occupied from step to step. This can lead to large variations in the density, causing the phenomenon known as charge sloshing¹⁵ where a fluctuating charge density from step to step is observed with insufficient attenuation to reach convergence.

In the present paper we transform the time-dependent Kohn-Sham equations of time-dependent density functional theory (TDDFT)¹⁶⁻¹⁸ to imaginary time¹⁹. We propose using these equations to propagate an initial state to very long imaginary time, refining it down to the KS state corresponding to its lowest energy component. The idea of using imaginary-time propagation (ITP) to find eigenstates is well-known, and it is frequently used to find ground state solutions to the Schrödinger equation describing single-particle systems with a fixed potential^{20,21}. It has also been employed in a DFT context as a performant alternative to the diagonalization step to find the single-particle KS eigenstates for a fixed electronic density, on a real space grid basis^{22,23}. However, the concept of imaginary-time evolution has yet to be examined as a stand-alone substitute to solving the KS equations through iterative density updating. In the present method both the density and wavefunction evolve together towards the ground state according to the Wick-rotated time-dependent Kohn-Sham equations, remaining consistent with each other throughout the calculation. Due to the density dependence of the KS Hamiltonian in the imaginary-time propagator, additional justifications of why we can expect the method to produce a ground state are required. We discuss the theoretical foundation of the imaginary-time evolution of the KS system, a procedure which is non-unitary, requiring re-orthonormalization of the states at each imaginary time-step. We show that the proof provided by van Leeuwen¹⁸ for TDDFT can be extended to imaginary-time time-dependent density functional theory (it-TDDFT), assuring in principle

that the density of a KS system will evolve in imaginary time in the same manner as the true many-body interacting system it models. The imaginary-time propagation method in DFT has attractive theoretical and practical benefits when applied to systems that are challenging to study using standard methods of solving the KS equation, as we will demonstrate.

First, we benchmark our procedure by applying it to the benzene molecule and show that the approach converges to the same ground state energy as other SCF-based methods. Next, we apply the it-TDDFT method to systems with known difficulties in achieving convergence. We chose to examine a copper nanocluster Cu_{13} with fixed magnetization and a spin-unpolarized Ru_{55} nanocluster. We show that self-consistent solutions are hard to realize in both systems using the most popular standard approach, SCF with Pulay mixing. In general, we find that while requiring more computation, our method is more dependable and more autonomous compared to SCF. It provides a good alternative to existing methodologies when the latter fails to converge in challenging systems, or if a user wishes to find an unfamiliar system's ground state with minimal manual intervention, particularly useful when a calculation is to be processed on a computing cluster.

Our paper is organized as follows. In Sec. II we present the general idea of the imaginary-time propagation method and how it can be applied to the time-dependent Kohn-Sham equations. In Sec. III we extend the van Leeuwen theorem to imaginary time, discuss theoretical aspects of the approach, and examine its relationship to the general SCF loop technique. We also propose the use of it-TDDFT as an alternative but equivalent way to define stationary states in the KS system, resulting in a definition better-suited for metallic and degenerate systems than the one presently used. In Sec. IV we show the results of calculations on the specific systems mentioned in the previous paragraph. Lastly, we conclude our findings in Sec. V.

II. THE METHOD

A. Imaginary-Time Propagation

First, let us consider the Hamiltonian as time-independent. Under the substitution $t \rightarrow -i\tau$, where τ is taken to be real, the time evolution operator transforms from $e^{-it\hat{H}}$ to $e^{-\tau\hat{H}}$. When $|\Phi_i\rangle$ is an eigenstate of \hat{H} , the time evolution of the eigenstate switches from rotating

its phase proportionally to its energy:

$$|\Phi_i(t)\rangle = e^{-it\hat{H}} |\Phi_i\rangle = e^{-itE_i} |\Phi_i\rangle, \quad (1)$$

to shrinking its amplitude by an exponential factor with a rate proportional to the energy:

$$|\Phi_i(\tau)\rangle = e^{-\tau\hat{H}} |\Phi_i\rangle = e^{-\tau E_i} |\Phi_i\rangle. \quad (2)$$

For the case of a time-dependent Hamiltonian the previous equations still hold for infinitesimal amounts of time Δt or $\Delta\tau$. For an arbitrary initial wavefunction $|\Psi(0)\rangle$, imaginary-time propagation amounts to

$$|\Psi(\tau)\rangle = \sum_{i=0}^{\infty} A_i(0) e^{-\tau E_i} |\Phi_i\rangle, \quad (3)$$

where $A_i(0)$ is the amplitude of the eigenstate component initially present. As imaginary time goes to infinity, $\tau \rightarrow \infty$, we see that the lowest initially present eigenstate $|\Phi_j\rangle$ (where j is the index corresponding to the lowest energy eigenvalue such that $A_j(0) \neq 0$), will dominate. We can choose to keep the state $|\Psi(\tau)\rangle$ normalized by dividing by the norm $\Omega(\tau) \equiv \sqrt{\langle\Psi(\tau)|\Psi(\tau)\rangle}$,

$$|\Psi(\tau)\rangle = \sum_{i=0}^{\infty} \frac{A_i(0) e^{-\tau E_i}}{\sqrt{\sum_{j=0}^{\infty} |A_j(0)|^2 e^{-2\tau E_j}}} |\Phi_i\rangle, \quad (4)$$

which then yields $\lim_{\tau \rightarrow \infty} |\Psi(\tau)\rangle = |\Phi_j\rangle$.

Note that the state $|\Psi(\tau)\rangle$ could be referring to a many-body state that has multiple position coordinates in real space, $\Psi(\mathbf{r}_1, \dots, \mathbf{r}_N)$. Since an arbitrary initial state generated by randomizing the coefficients in some basis is very likely to have a nonzero ground state component, ITP can be used to find ground state wavefunctions and energies.

B. Implementation within the Kohn-Sham Formalism

In time-dependent density functional theory, starting from an initial state, the Kohn-Sham system in atomic units obeys the equation of motion

$$i \frac{\partial}{\partial t} \phi_j(\mathbf{r}, t) = \hat{H}_{\text{KS}}[n(\mathbf{r}, t)] \phi_j(\mathbf{r}, t), \quad (5)$$

$$\hat{H}_{\text{KS}}[n(\mathbf{r}, t)] \equiv \left[-\frac{\nabla^2}{2} + v_s(\mathbf{r}, t) \right], \quad (6)$$

with time-dependent effective potential

$$v_s[n(\mathbf{r}, t)] = v(\mathbf{r}) + v_{\text{H}}[n(\mathbf{r}, t)] + v_{\text{xc}}[n(\mathbf{r}, t)]. \quad (7)$$

In these expressions, $v(\mathbf{r})$ is the external potential and

$$v_{\text{H}}[n(\mathbf{r}, t)] = \int d\mathbf{r}' \frac{n(\mathbf{r}', t)}{|\mathbf{r} - \mathbf{r}'|}, \quad (8)$$

$$v_{\text{xc}}[n(\mathbf{r}, t)] = \frac{\delta E_{\text{xc}}[n(\mathbf{r}, t)]}{\delta n(\mathbf{r}, t)}, \quad (9)$$

$$n(\mathbf{r}, t) = \sum_{j=1}^N |\phi_j(\mathbf{r}, t)|^2. \quad (10)$$

The Kohn-Sham time-evolution can be reformulated in terms of a time-propagator which acts on single-particle states and is given by

$$|\phi_j(t)\rangle = \hat{U}(t, t_0) |\phi_j(t_0)\rangle, \quad (11)$$

$$\hat{U}(t, t_0) = \hat{\mathcal{T}} \exp \left(-i \int_{t_0}^t \hat{H}_{\text{KS}}[n(\mathbf{r}, t')] dt' \right), \quad (12)$$

where $\hat{\mathcal{T}}$ is the time-ordering operator. In imaginary time, applying the substitution $t \rightarrow -i\tau$ results in

$$|\phi_j(\tau)\rangle = \hat{\mathcal{U}}(\tau, \tau_0) |\phi_j(\tau_0)\rangle, \quad (13)$$

$$\hat{\mathcal{U}}(\tau, \tau_0) = \hat{\mathcal{T}}_\tau \exp \left(- \int_{\tau_0}^{\tau} \hat{H}_{\text{KS}}[n(\mathbf{r}, \tau')] d\tau' \right), \quad (14)$$

where $\hat{\mathcal{T}}_\tau$ now time-orders in imaginary time. Note that the imaginary-time propagator is

not unitary. The time-dependent KS Eq.6 becomes a diffusion equation:

$$-\frac{\partial}{\partial\tau}\phi_j(\mathbf{r},\tau) = \hat{H}_{\text{KS}}[n(\vec{r},\tau)]\phi_j(\mathbf{r},\tau). \quad (15)$$

Employing the same numerical scheme used for real time propagation of KS states on an atomic basis as Ref. 24, we imaginary-time evolve the single-particle states using finite time steps $\Delta\tau$ and the instantaneous imaginary-time propagator is approximated with the second-order Magnus expansion:

$$\hat{\mathcal{U}}(\tau + \Delta\tau, \tau) \approx \exp \left[-\Delta\tau \hat{H}_{\text{KS}} \left(\tau + \frac{\Delta\tau}{2} \right) \right], \quad (16)$$

$$\hat{H}_{\text{KS}}(\tau) \equiv \hat{H}_{\text{KS}}[n(\mathbf{r}, \tau)]. \quad (17)$$

The Hamiltonian at the midpoint is approximated as the average of the Hamiltonians at τ_i and τ_{i+1} , $\hat{H}_{\text{KS}}(\tau_i + \frac{\Delta\tau}{2}) \approx \frac{1}{2} [\hat{H}_{\text{KS}}(\tau_i) + \hat{H}_{\text{KS}}(\tau_{i+1})]$. Each step is iterated to self-consistency in order to make use of the Hamiltonian at τ_{i+1} . We use the Padé rational polynomial approximation of arbitrary degree to obtain the general matrix exponential. Further details of the numerical propagation can be found in Ref. 24, which describes TDAP-2.0, a TDDFT code we used, built on top of SIESTA²⁵, a DFT package which uses strictly localized basis sets. While the midpoint Hamiltonian greatly aids stability and energy conservation in real time propagation, in practice we have found that for imaginary-time propagation we can just use the first step in the iterative procedure, which simply applies the approximation $\hat{H}_{\text{KS}}(\tau_i + \frac{\Delta\tau}{2}) \approx \hat{H}_{\text{KS}}(\tau_i)$. This explicit propagation is faster since the Hamiltonian only needs to be evaluated once per propagation step, and the effect on the size of the maximum stable time-step appears negligible compared to the implicit method using the midpoint Hamiltonian. This is expected since imaginary-time propagation is inherently more stable than the real-time propagation the TDAP-2.0 code was originally designed to solve.

Because the imaginary-time propagator is not unitary, the single-particle states lose their normalization and generally cease to be orthogonal. The simple expression for density in Eq. 10 becomes more complicated if the single-particle states ϕ_j are non-orthonormal. So, it is convenient to reorthonormalize the single-particle states each time step. It turns out that the particulars of how the orthogonalization is achieved do not affect the physics, as we will show in Section III B. We use the modified Gram-Schmidt algorithm to orthonormalize

the states.

While we used a localized atomic basis for our calculations, the method we propose is independent of the basis used to represent the Kohn-Sham orbitals. Given a plane-wave or gaussian DFT package which already supports real-time propagation using TDDFT, it is straightforward to implement it-TDDFT, employing appropriate numerical methods for orthonormalization in those bases.

III. THEORETICAL CONSIDERATIONS

A. Monotonically Decreasing Energy

The imaginary time discussion in Section II A assumed that the Hamiltonian was time independent, and using its unchanging eigenvalues and eigenstates we showed that it purifies a random wavefunction into its lowest-energy component. However, in the Kohn-Sham system the Hamiltonian depends on the density, and thus will in general have eigenenergies and eigenvalues that depend on time. In particular, for the density at time τ_ℓ , $n(\mathbf{r}, \tau_\ell)$, we are considering a quantum system with the Hamiltonian $\hat{H}_{\text{KS}}[n(\mathbf{r}, \tau_\ell)]$. By propagating the state of interest in imaginary time using this instantaneous Hamiltonian, we are amplifying the low-energy eigenstates of the current Hamiltonian $\hat{H}_{\text{KS}}[n(\tau_\ell)]$, which in general are different than the low-energy eigenstates of the new Hamiltonian, $\hat{H}_{\text{KS}}[n(\tau_{\ell+1})]$. While it seems plausible that this process always decreases the energy of an arbitrary state given that at every time-step the amplitudes of the state's high energy components are reduced, this reasoning alone turns out to be insufficient. Since the eigenstates of the new Hamiltonian $\hat{H}_{\text{KS}}[n(\tau_{\ell+1})]$ differ from the previous ones, the resultant state following a propagation step could conceivably have a higher energy than the previous state. A good example of this is the commonly-observed divergence of SCF loops without a mixing scheme. In such a setup, on the i th step the N -lowest eigenstates of the Hamiltonian $\hat{H}_{\text{KS}}[n_i]$ are filled and are directly used to compute the next density n_{i+1} . In a diverging scenario, computing the energy of the present state given the new density n_{i+1} gives a higher energy than in the previous step, permitted by the fact that the present state was created as the ground state of $\hat{H}_{\text{KS}}[n_i]$ and not of $\hat{H}_{\text{KS}}[n_{i+1}]$. This example also reveals an interesting limiting case of it-TDDFT. If a KS state is propagated to infinite imaginary time before the density used

in the instantaneous Hamiltonian $\hat{H}_{\text{KS}}[n(\tau_\ell)]$ is updated, the propagated state will become the ground state of the present Hamiltonian, which is equivalent to populating the N -lowest eigenstates of $\hat{H}_{\text{KS}}[n(\tau_\ell)]$. In this way basic SCF can be thought of as it-TDDFT with infinitely large time-steps when using explicit propagation. Indeed, if the time-step in it-TDDFT is taken to be too large, the total energy will diverge, just like in SCF performed without a mixing scheme.

With a reasonable time-step (usually around $1\hbar/\text{Ry}$ or smaller), it turns out that it-TDDFT does actually monotonically decrease the total energy of the system. The van Leeuwen theorem¹⁸ provides the theoretical backbone for this result, requiring only a minor extension to account for imaginary time as we will demonstrate in the following sections. The van Leeuwen theorem guarantees that given the exact effective single-particle potential, the Kohn-Sham system produces a time-dependent density that matches the density of the true interacting system. Typically this result is implicitly used to assert that results calculated in the Kohn-Sham system can be applied to the fully interacting system, but we will instead employ the theorem in the other direction. While propagation of the Kohn-Sham system is complicated by the dependence on density, in the true interacting system the evolution in imaginary time has the simple form given in Eq. 4. In this equation it is clear that the energy of an eigenstate remains constant, while the energy of an arbitrary state with multiple components will strictly decrease with τ towards the energy of the lowest present eigenstate. Given that the total energy of the system is a functional of density, by the equality of the two densities granted by the van Leeuwen theorem, the total energy in the Kohn-Sham system will also converge to the energy of the lowest-energy component present in the initial state.

B. Maintaining Orthonormalization

In general, imaginary-time propagation will change the norm of a wavefunction. While we can manually account for this by dividing the wavefunction by its norm whenever we need to compute an observable, it is not obvious that this operation, or the proposed re-orthogonalization of the single-particle wavefunctions, is compatible with the van Leeuwen theorem. However, it turns out that orthonormalization of the single-particle states is equivalent to adding a purely time-dependent function $\lambda(t)$ to the many-body Hamiltonian. We

will show that in imaginary time this takes care of holding the wavefunction normalized, both in the interacting and Kohn-Sham systems, as well as accounting for the orthogonalization step we use in the Kohn-Sham state propagation. With this addition, time t can be taken to be imaginary in the van Leeuwen proof with hardly any modifications, as shown in the next section.

To understand the importance of $\lambda(t)$ in imaginary-time propagation, let us first consider its effect in the interacting system. In real time propagation, the choice of $\lambda(t)$ does not affect the dynamics of density since this spatially-constant offset in energy only results in changing the phase of the wavefunction. Explicitly, we see that

$$\begin{aligned} |\Psi(t)\rangle &= \hat{U}(t, t_0) |\Psi(t_0)\rangle, \\ \hat{U}(t, t_0) &= \hat{\mathcal{T}} \exp \left(-i \int_{t_0}^t \hat{H}(t') + \lambda(t') dt' \right) \\ &= \hat{U}_\lambda(t, t_0) \hat{\mathcal{T}} \hat{U}_{\hat{H}}(t, t_0), \end{aligned} \tag{18}$$

$$\hat{U}_\lambda(t, t_0) \equiv \exp \left(-i \int_{t_0}^t \lambda(t') dt' \right), \tag{19}$$

$$\hat{U}_{\hat{H}}(t, t_0) \equiv \exp \left(-i \int_{t_0}^t \hat{H}(t') dt' \right). \tag{20}$$

However, in imaginary-time propagation, $\lambda(\tau)$ now modifies the imaginary-time propagator $\hat{\mathcal{U}}(\tau, \tau_0)$ by a time dependent magnitude,

$$\hat{\mathcal{U}}(\tau, \tau_0) = \hat{\mathcal{U}}_\lambda(\tau, \tau_0) \hat{\mathcal{T}}_\tau \hat{\mathcal{U}}_{\hat{H}}(\tau, \tau_0), \tag{21}$$

$$\hat{\mathcal{U}}_\lambda(\tau, \tau_0) \equiv \exp \left(- \int_{\tau_0}^\tau \lambda(\tau') d\tau' \right), \tag{22}$$

$$\hat{\mathcal{U}}_{\hat{H}}(\tau, \tau_0) \equiv \exp \left(- \int_{\tau_0}^\tau \hat{H}(\tau') d\tau' \right). \tag{23}$$

If this $\lambda(\tau)$ is arbitrary, the norm of the wavefunction will change in time, incorrectly scaling the expectation values of observables like density and energy. The norm of the wavefunction can be held fixed by choosing $\lambda(\tau)$ to counteract the norm-altering effect of $\hat{\mathcal{T}}_\tau \exp \left(- \int_{\tau_0}^\tau \hat{H}(\tau') d\tau' \right)$ when it acts on $|\Psi(\tau_0)\rangle$. Note that such a $\lambda(\tau)$ will also depend on the starting state. For example, in the time-independent Hamiltonian case presented in

Section II A, from Eq. 4 we see that

$$\hat{\mathcal{U}}_\lambda(\tau, \tau_0) = \left[\sum_{j=0}^{\infty} |A_j(0)|^2 e^{-2\tau E_j} \right]^{-1/2} \quad (24)$$

which implies that

$$\lambda(\tau) = \frac{1}{2} \frac{d}{d\tau} \ln \left[\sum_{j=0}^{\infty} |A_j(0)|^2 e^{-2\tau E_j} \right] = -\langle E(\tau) \rangle. \quad (25)$$

The final equality also gives us some intuition about the task we impose on $\lambda(\tau)$: it subtracts away the average energy of our present state. In other words, to keep the wavefunction normalized, the energies of the Hamiltonian must be measured relative to $\langle E(\tau) \rangle$. This result holds more generally for time-dependent Hamiltonians as well, which can be shown by using $\hat{\mathcal{U}}(\tau, \tau_0)$ from Eq. 21 and differentiating the norm-conserving equation $1 = \langle \Psi(\tau_0) | \hat{\mathcal{U}}^\dagger(\tau, \tau_0) \hat{\mathcal{U}}(\tau, \tau_0) | \Psi(\tau_0) \rangle$ to solve for $\lambda(\tau)$. We will assume that such a $\lambda(\tau)$ is used in the interacting system so that the system always remains normalized. Now we will look at this concept in the corresponding Kohn-Sham system.

In the Kohn-Sham system the propagator is given by

$$\hat{\mathcal{U}}(\tau, \tau_0) = \hat{\mathcal{U}}_{\lambda_{\text{KS}}}(\tau, \tau_0) \hat{\mathcal{T}}_\tau \hat{\mathcal{U}}_{\hat{H}_{\text{KS}}}(\tau, \tau_0). \quad (26)$$

where \hat{H}_{KS} is understood to act on the entire Kohn-Sham many-body wavefunction $|\Phi\rangle$ by acting on its constituent single-particle states $|\phi_j\rangle$ according to Eq. 6. In general $\lambda_{\text{KS}}(\tau)$ differs from the constant $\lambda(\tau)$ present in the interacting system, and in addition to normalizing the many-body state, it can account for orthonormalization of the constituent single-particle states.

In the it-TDDFT method we describe in this paper, we orthonormalize the Kohn-Sham single-particle wavefunctions after every imaginary time-step. We will show that this procedure amounts to a choice of norm-conserving $\lambda_{\text{KS}}(\tau)$, which does not interfere with the dynamics. First we consider the effect of an invertible transformation on the single-particle wavefunctions in a single-Slater-determinant wavefunction.

Suppose we have single-Slater-determinant many-body wavefunction $\Phi(\mathbf{r}_1, \mathbf{r}_2, \dots, \mathbf{r}_N) =$

$\frac{1}{\sqrt{N!}} \det\{\mathbf{A}\}$, where

$$\mathbf{A} = \begin{pmatrix} \phi_1(\mathbf{r}_1) & \phi_2(\mathbf{r}_1) & \cdots & \phi_N(\mathbf{r}_1) \\ \phi_1(\mathbf{r}_2) & \phi_2(\mathbf{r}_2) & \cdots & \phi_N(\mathbf{r}_2) \\ \vdots & \vdots & \ddots & \vdots \\ \phi_1(\mathbf{r}_N) & \phi_2(\mathbf{r}_N) & \cdots & \phi_N(\mathbf{r}_N) \end{pmatrix}. \quad (27)$$

Consider a new many-body wavefunction $\tilde{\Phi}(\mathbf{r}_1, \mathbf{r}_2, \dots, \mathbf{r}_N)$ composed of single-particle wavefunctions $\{\tilde{\phi}_i\}$ reached by an invertible transformation \mathbf{S} within the space spanned by $\{\phi_i\}$, which transforms the single-particle states according to $\tilde{\phi}_i(\mathbf{r}) = \sum_{j=1}^N \phi_j(\mathbf{r}) S_{ji}$. We then have that $\tilde{\Phi}(\mathbf{r}_1, \mathbf{r}_2, \dots, \mathbf{r}_N) = \frac{1}{\sqrt{N!}} \det \tilde{\mathbf{A}}$, where $\tilde{A}_{ik} = \tilde{\phi}_k(\mathbf{r}_i) = \sum_{j=1}^N \phi_j(\mathbf{r}_i) S_{jk} = \sum_{j=1}^N A_{ij} S_{jk} = (AS)_{ik}$, which implies $\tilde{\mathbf{A}} = \mathbf{A}\mathbf{S}$. Thus, $\tilde{\Phi}(\mathbf{r}_1, \mathbf{r}_2, \dots, \mathbf{r}_N) = \frac{1}{\sqrt{N!}} \det(\mathbf{A}\mathbf{S}) = \frac{1}{\sqrt{N!}} \det(\mathbf{A}) \det(\mathbf{S}) = \det(\mathbf{S}) \Phi(\mathbf{r}_1, \mathbf{r}_2, \dots, \mathbf{r}_N)$, meaning that the two wavefunctions differ by at most a complex scalar. Any possible orthonormalization of the occupied single-particle states is an invertible transformation as it preserves the subspace spanned by these linearly-independent states, so we see from the above that this process merely amounts to changing the phase and rescaling the many-body wavefunction.

At the starting time τ_0 , we assume the Kohn-Sham wavefunction is properly normalized. Following the application of the imaginary-time propagator up to a particular time τ , we represent a particular orthonormalization of the single-particle states by an invertible transformation $\mathbf{S}(\tau)$. In order for $\lambda_{\text{KS}}(\tau)$ to act like the orthonormalization procedure, we require that

$$\hat{\mathcal{U}}_{\lambda_{\text{KS}}}(\tau, \tau_0) = \det\{\mathbf{S}\}(\tau). \quad (28)$$

Note that $|\det S(\tau)|$ will be continuous since it is the reciprocal of the norm of the unnormalized propagated wavefunction. The phase of $\det S(\tau)$ is not important to match since it just amounts to changing the phase of the wavefunction, which will not affect the density. As such, we are free to use any orthonormalization procedure at each time-step without concern about the continuity of the phase, and a purely real $\lambda_{\text{KS}}(\tau)$ satisfying $\hat{\mathcal{U}}_{\lambda_{\text{KS}}}(\tau, \tau_0) = |\det\{\mathbf{S}\}(\tau)|$ for all $\tau > \tau_0$ is guaranteed to exist.

This defines an energy shift we can use in the Kohn-Sham system to hold the norm at unity

throughout the propagation. Using $\lambda(\tau)$ and $\lambda_{\text{KS}}(\tau)$, only minor modifications are required to extend the van Leeuwen theorem¹⁸ to imaginary time, as shown in the next section. This is a powerful result since it allows us to think about imaginary-time propagation in the Kohn-Sham system in terms of what it does in the real system, allowing the Wick-rotation connections from quantum mechanics to statistical mechanics to be employed. For example, it justifies the use of the Kohn-Sham system as a stand-in for the interacting system in our calculations performed for imaginary time path integrals¹⁹.

C. Van Leeuwen Theorem in Imaginary Time

In Ref. 18 van Leeuwen shows that a time-dependent particle density $n(\mathbf{r}, t)$ belonging to a many-particle system with two-particle interaction \hat{W} can always be reproduced by a unique (up to an additive purely time-dependent constant) external potential $v'(\mathbf{r}, t)$ in another many-particle system that uses a different two-particle interaction \hat{W}' , under the mild restriction that the density has to be analytic in time. If we choose the two-particle interaction in this other system to simply be no interaction, *i.e.* $\hat{W}' = 0$, the theorem guarantees the existence of the effective potential $v_s(\mathbf{r}, t)$ for a Kohn-Sham system that reproduces the same time-dependent density as the interacting system of interest. For this section, we will closely follow van Leeuwen's original paper and note the modifications that need to be made to make it compatible with imaginary-time evolution and the specifics discussed in Section III B.

First of all, treating time t as complex does not pose any problems with the operations performed in the proof, where t appears in some time derivatives but otherwise is treated as a parameter. The only remaining concern is that the possibly changing norm of the wavefunction could affect the density and other observables appearing in the differential equations underpinning the result. To avoid such issues, we simply need to fit our specific choice of norm-conserving $\lambda(t)$, discussed in the previous section, into the framework of the proof to make it compatible with it-TDDFT. The van Leeuwen proof uses the formalism of second quantization, writing the Hamiltonian \hat{H} of a finite many-particle system as

$$\hat{H}(t) = \hat{T} + \hat{V}(t) + \hat{W} + \lambda(t), \quad (29)$$

where

$$\hat{T} = -\frac{1}{2} \int d^3\mathbf{r} \hat{\psi}^\dagger(\mathbf{r}) \nabla^2 \hat{\psi}(\mathbf{r}), \quad (30)$$

$$\hat{V}(t) = \int d^3\mathbf{r} v(\mathbf{r}t) \hat{\psi}^\dagger(\mathbf{r}) \hat{\psi}(\mathbf{r}), \quad (31)$$

$$\hat{W} = \int d^3\mathbf{r} d^3\mathbf{r}' w(|\mathbf{r} - \mathbf{r}'|) \hat{\psi}^\dagger(\mathbf{r}) \hat{\psi}^\dagger(\mathbf{r}') \hat{\psi}(\mathbf{r}') \hat{\psi}(\mathbf{r}), \quad (32)$$

and we add on our time-dependent constant $\lambda(t)$. Because it is simply a scalar, it does not affect any of the commutators involving $\hat{H}(t)$ in the Heisenberg equations of motion of various observables appearing in the proof. There is only one more detail to note, regarding the freedom to add an arbitrary $C(t)$ to the potential of the primed system, $v'(\mathbf{r}, t)$, in the original proof. From Eq. 31 we see that such a time-dependent constant modifies the Hamiltonian by an additional term $C(t)\hat{N}$, where \hat{N} is the number operator. For the systems of interest, the number of particles is fixed at N so we see that $C(t)N$ functions mathematically like $\lambda'(t)$. This just means that a norm-conserving $\lambda'(t)$ will cancel out any effect from the choice of $C(t)$. Thus, with $\lambda(t)$ and $\lambda'(t)$ properly chosen to ensure that the norm of states in both the unprimed and primed systems is held at unity, both guaranteed to exist as discussed in Section III B, the van Leeuwen theorem holds in imaginary time.

D. it-TDDFT as an Alternative Theoretical Foundation for Stationary States in DFT

The first step in the vast majority of DFT calculations is to find a density corresponding to a stationary state, *i.e.* a ground or excited state, of the many-body interacting system. A stationary state can be identified as an eigenstate of the Hamiltonian, or equivalently, as a state that only changes by a phase when evolved in real time or by a multiplicative factor when evolved in imaginary time. These two definitions are likewise applicable to the Kohn-Sham system used in DFT, but only the first is widely used at present, given the ubiquitous use of SCF. In systems that are difficult to converge with SCF, owing to their size or metallic character, the second definition becomes useful when paired with the it-TDDFT method.

The standard approach for defining when we have found a density corresponding to a stationary state of the interacting system is through the Kohn-Sham equations. The Kohn-

Kohn-Sham equations are set as an eigenvalue problem, and once a density $n(\mathbf{r})$ is found such that a choice of N of the single-particle eigenfunctions $\phi_j(\mathbf{r})$ reproduces the same density through Eq. 10, a stationary state has been determined. To arrive at such solutions, we usually use SCF to find ground states, where the N lowest-energy eigenstates are chosen, and Δ SCF²⁶, where some other selection of N single-particle eigenstates is chosen to represent an excited state. Typically, for small systems, insulating systems, and systems with low degeneracy of single-particle states, after a few steps of the SCF iterative process with a mixing scheme, the eigenstates rarely change order when sorted by energy from one step to the next. This means that the single-particle states chosen to be occupied have similar character to those from the step before, so the resulting density is not too different from the previous step. In these cases SCF converges well so it makes sense to use the satisfaction of the time-independent Kohn-Sham equations as the theoretical justification that the obtained density is that of a stationary state. However, in large systems and in metallic systems, or if an excited state is desired, SCF and Δ SCF methods can struggle to converge. The small differences in eigenenergies of the single-particle states, as well as the presence of many states near the Fermi level or the highest occupied state in the case of excited systems, can cause very different eigenstates to be occupied from step to step. This leads to large variations in the density, causing the phenomenon known as charge sloshing. In principle, if an exactly correct stationary state density is known, the fact that the Kohn-Sham equations are satisfied can still be used as the justification that the density indeed corresponds to a stationary state's. In practice, however, this route becomes less useful in these difficult systems since even a density that is very nearly correct could appear to be far from convergence if the wrong single-particle states are chosen to be occupied, resulting in a very different density from the one given. In addition, this makes it challenging to discern whether a non-converging density is acceptably close for subsequent calculations, or if it is completely off mark. For example, in Section IV D we examine the performance of SCF on a ruthenium nanocluster, where we show in Table I that some non-converged densities give a reasonable energy estimate for the ground state, while others are unusably incorrect.

To address convergence issues, DFT calculations of metallic systems and systems with high single-particle state degeneracy are often performed with electronic smearing¹¹, where the states near the Fermi level are given fractional occupations to simulate nonzero electronic temperature. This mitigates the issue with consecutive SCF steps choosing very different

single-particle states by ensuring that states near each other in energy have similar fractional occupation. Smearing adds an entropic contribution to the energy, so a balance between obtaining an accurate energy and ease of convergence has to be struck. Furthermore, as electronic smearing is a computational tool and not intended to be an accurate representation of the effects of temperature, in principle once convergence is obtained with a certain amount of smearing, the effect should be incrementally reduced until the solution with no smearing is achieved¹⁰. In fact, cases have been found where even small amounts of electronic smearing produced significantly different results from the same calculation performed with integer occupations, such as a HOMO-LUMO gap energy that differed by one order of magnitude²⁷. As we show with the ruthenium nanocluster in Section IV D, achieving convergence even while applying electronic smearing can still require some finesse and guesswork.

In systems where SCF convergence is hard to attain, instead of using the time-independent Kohn-Sham equations to show that a state is stationary, we can use its invariance under imaginary-time evolution. If a Kohn-Sham wavefunction stays constant when propagated in imaginary time, then its single-particle states span the same subspace as a set of eigenstates of the Kohn-Sham Hamiltonian evaluated with the present density. The converse is true as well, namely that a set of N states satisfying the time-independent Kohn-Sham equations will be invariant under imaginary-time evolution, ignoring the possibly changing norm which can be corrected by a time-dependent energy shift. Thus, finding a Kohn-Sham many-body state $|\Phi(\tau_0)\rangle$ that stays the same when propagated in imaginary time, $|\Phi(\tau)\rangle = \hat{\mathcal{U}}(\tau, \tau_0) |\Phi(\tau_0)\rangle = |\Phi(\tau_0)\rangle$, where the Hamiltonian in the imaginary-time propagator $\hat{\mathcal{U}}$ contains an orthonormality-preserving $\lambda(\tau)$, is equivalent to finding a set of constituent N single-particle states that satisfy the time-independent Kohn-Sham equations.

This definition of what qualifies as a stationary state has a few advantages. In systems where the single-particle states are close in energy, the charge-sloshing issue of not filling the “same” states from one numerical step to the next is eliminated. In it-TDDFT the occupied orbitals are followed throughout their evolution so there is no need to devise methods like electronic smearing to deal with the ambiguity of the appropriate states to fill. Similarly, systems that have degenerate states pose no problem for it-TDDFT since it will simply converge to one of the states in the subspace without needing to occupy all the degenerate states equally.

E. Practical Advantages of it-TDDFT

SCF-loop-based approaches will generally arrive at a stationary state faster than imaginary-time propagation since it-TDDFT needs to maintain self-consistency between the electronic state and the density used in the KS Hamiltonian the entire calculation. However, the it-TDDFT method has computational advantages of its own.

One convenience afforded by it-TDDFT is that a user only needs to choose a single parameter when attempting to converge a system, the time-step. Compare this to the various parameters usually required for mixing schemes used with SCF, where in some systems there are sets of parameter choices that do not result in convergence. Even when the chosen parameters do succeed, there are systems where different stationary states can be obtained even for slight variations in the mixing parameters, as shown in the case of a Cu_{13} cluster in Section IV C. In contrast, convergence in the it-TDDFT method is not very sensitive to the choice of time-step. In a proper numerical implementation of it-TDDFT, any time-step that is smaller than a convergent time-step will also result in convergence, and more stringently, will lead to the same density trajectory in imaginary time given the same starting state. This property allows us to readily remove this parameter choice if desired through algorithms that can automatically adjust the time-step on the fly, further simplifying the use of the it-TDDFT method. For example, for the it-TDDFT calculations done in Sections IV C and IV D, we employed a very basic automated time-step. We increased the time-step by 10% every step until the energy no longer decreased, at which point we would immediately set the time-step back to its safe starting value, letting it increase again. A more purposive algorithm would likely be more efficient, although we found that this simplistic procedure performed as well as manually searching for a static time-step that is as large as possible while still resulting in convergence.

Another practical advantage of using imaginary-time evolution is that not-yet-converged states still have physical meaning. At any given time, the single-particle states and the electronic density used in the KS Hamiltonian are self-consistent, and in principle this density trajectory is equal to the imaginary-time evolving density of the interacting system, by the van Leeuwen theorem. Through this connection, the partially-converged KS state corresponds to a superposition of a dominant ground state component and a few low-amplitude excited states, in the interacting system. As such, even before the it-TDDFT calculation

of the ground state has terminated according to user-specified energy or density difference tolerances, approximate ground state observables can be calculated. This property can allow for preliminary calculations of band structure, energies, optical properties, or atomic forces to proceed while the ground state calculation continues to be refined. In contrast, there are no guarantees of validity for observables calculated from intermediate states produced in a SCF loop since they are not self-consistent with the density used in the functional, and potentially very far from the correct KS ground state.

When an SCF loop ceases to make progress, failing to decrease the density difference between steps, not much is gained aside from the knowledge that the particular set of mixing parameters, amount of electronic smearing, and position of the atoms used in the calculation did not work. It could take a substantial amount of tweaking of these parameters before chancing upon a set that results in convergence. This can be time-consuming and a frustrating use of computing resources given that these exploratory runs do not produce usable results. This highlights another strength of it-TDDFT, since calculation time dedicated to it will always improve the quality of the state at hand, even if the gain is minor. It is also straightforward to continue a calculation from a saved state, so the method is amenable to successive runs on a remote computing cluster.

In our discussion we have assumed that we are performing DFT with a Kohn-Sham system, which uses a single Slater determinant. It should be possible to apply it-TDDFT for finding stationary states in other approaches which use linear combinations of Slater determinants, or ensemble DFT, owing to the method’s physically-motivated working principle. A proper theory meant to reproduce the same density trajectory as the true interacting system should converge an arbitrary starting state in a DFT model system to a stationary state when propagated in imaginary time.

F. Power Iteration and Other Propagators

As a final note for the theoretical discussion, imaginary-time propagation, in its numerical implementation, resembles power iteration, a method in applied mathematics for finding the dominant eigenvalue of a matrix, and a corresponding eigenvector. Specifically, the relevant matrix is $\exp(-\hat{H}_{\text{KS}}[n]\Delta\tau)$, which has maximal eigenvalue $\exp(-\epsilon_0\Delta\tau)$ where ϵ_0 is the lowest eigenenergy of the Hamiltonian at the present density. Because the imaginary-time prop-

agator is a matrix function of \hat{H}_{KS} , it shares the same eigenvectors as the Hamiltonian. So, if we find the maximal eigenvalue of the propagator, we also obtain an eigenstate of the system. Power iteration converges geometrically with ratio $|\lambda_2/\lambda_1|$, where λ_1 is the dominant eigenvalue, and λ_2 is the second dominant eigenvalue. As such, it is tempting to use a different “propagator”, a matrix function of the Hamiltonian $f(\hat{H}_{\text{KS}})$ which more strongly separates eigenvalues in order to increase the rate of convergence. However, this idea is foiled by the complication discussed earlier in this section, the Hamiltonian’s dependence on density. The larger the change in density for a given power iteration step, the less the new Hamiltonian resembles what it did in the previous step, leading to instability. For example, simply using a larger time-step $\Delta\tau$ decreases the ratio $|\lambda_2/\lambda_1| = |\exp(-\epsilon_1\Delta\tau)/\exp(-\epsilon_0\Delta\tau)|$, which for a fixed matrix would increase the rate of convergence. However, as stated in Section III A, due to the Hamiltonian’s dependence on density a large time-step generally leads to instability and a breakdown of the method. Furthermore, using a different propagator loses us the van Leeuwen connection to the real interacting system, and with it the guarantee of monotonically decreasing total energy.

IV. EXAMPLE CALCULATIONS

A. Density Distance to Ground State

In order to compare two different densities, it is useful to have a measure of distance. There are various ways to do this, but we will use the L^1 distance divided by two for its intuitive physical meaning when applied to densities. Half the L^1 distance between two density distributions is given by

$$D[n, n_0] \equiv \frac{1}{2}d_1(n, n_0) = \frac{1}{2} \int |n(\mathbf{r}) - n_0(\mathbf{r})| d^3\mathbf{r}, \quad (33)$$

which can be interpreted as the number of electrons in the wrong place relative to the reference density n_0 . This can be seen by using the fact that both densities integrate to the same value, the total number of electrons. The regions of excess density relative to n_0 contain electrons that are “out of place” since they are supposed to be where the density is lacking relative to n_0 . The integral of the absolute value of the density difference over all

space adds up the excess density and the negative of the lacking density, both contributing equally, so we have to divide by two to obtain the number of electrons out of place.

B. Benzene Ground State Calculation

As a demonstration of how the ground state is determined using it-TDDFT, we apply the method to a benzene molecule. We also show that it produces the same density and energy as a standard SCF calculation. The atomic coordinates were first optimized by employing the conjugate gradient method using standard SCF to find the electronic ground states of trial atomic configurations. We could have also used it-TDDFT to calculate ground states of these intermediate atomic configurations in the geometry optimization.

In the system with relaxed atomic positions, we initialized the single-particle electronic states by randomly sampling basis coefficients from a uniform distribution, where the basis used consists of localized atomic orbitals. Then, to obtain a proper state we orthonormalized the single-particle wavefunctions. Propagating this initial state in imaginary time, we eventually obtain the same ground state as determined by an SCF approach with Pulay mixing. The Kohn-Sham energy and the density distance of the propagated state are plotted as a function of imaginary time in Figure 1, both computed relative to the SCF-determined ground state. As both these quantities asymptote to effectively zero in the context of their numerical implementations, this shows that it-TDDFT produces a Kohn-Sham state that has the same energy and density as the ground state determined with a standard SCF approach. As one would expect, switching the method to SCF at the end of the imaginary-time propagation reports SCF convergence after the first step.

C. Copper Nanocluster with Fixed Magnetization

The system of a Cu_{13} nanocluster was considered by Hoyt et al. in Ref. 28 in its ground state magnetization of $m = 5\mu_B$ and excited state $m = 3\mu_B$. In discussions the authors indicated that the $m = 1\mu_B$ excited state was tricky to converge, making it a good candidate for the it-TDDFT method.

In Figures 2 and 3, we present the main results of our computations for the self-consistent KS states with $m = 1\mu_B$ magnetization, which has total spin 1/2. Additional information

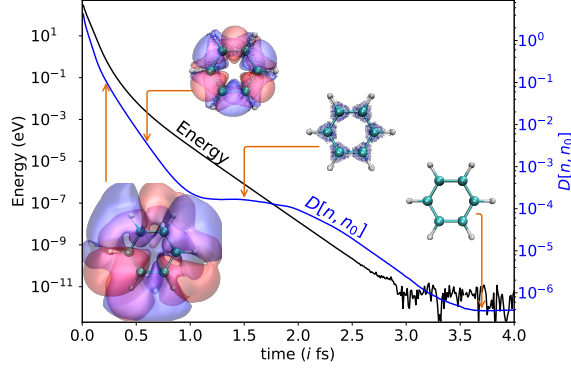


FIG. 1: Determining the ground state of benzene using it-TDDFT. The time step used was 10.0 as. The black curve shows the Kohn-Sham energy of a randomized electronic starting state propagated in imaginary time measured relative to the ground state energy determined with SCF. The blue curve shows the density distance $D[n, n_0]$, which is interpreted as the number of electrons out of place relative to the ground state, as a function of imaginary time. Fixed positive and negative isosurfaces of the density difference $n(\mathbf{r}) - n_0(\mathbf{r})$ are shown at various points in the propagation.

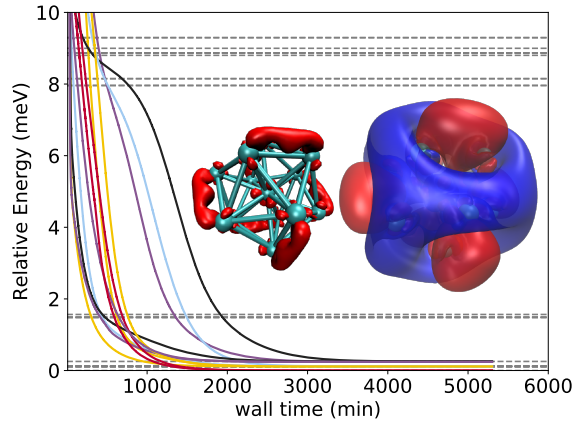


FIG. 2: Electronic energy of Cu_{13} with fixed spin polarization $+1/2$, relative to the lowest energy obtained with this fixed polarization. Each solid line is an energy trajectory produced by propagating a random initial state in imaginary time, plotted versus the wall time taken to perform the calculation on 4 cores on an Intel Xeon Gold 6140. The five possible colors of the solid lines indicate which of the five rotationally-equivalent lowest-energy states the given system converges to. On the right, the spin magnetization density of one such state is shown, with spin up and spin down designated by blue and red respectively. On the left, only a spin down isosurface is presented to better exhibit the five-fold symmetry of the lowest energy states. The dashed lines show the relative energies of converged states obtained using SCF and Pulay mixing with different parameters as detailed in Figure 3 and Table II. Notice that it-TDDFT consistently converges to one of the lowest energy states regardless of the random starting state while SCF converges to various states depending on the mixing parameters.

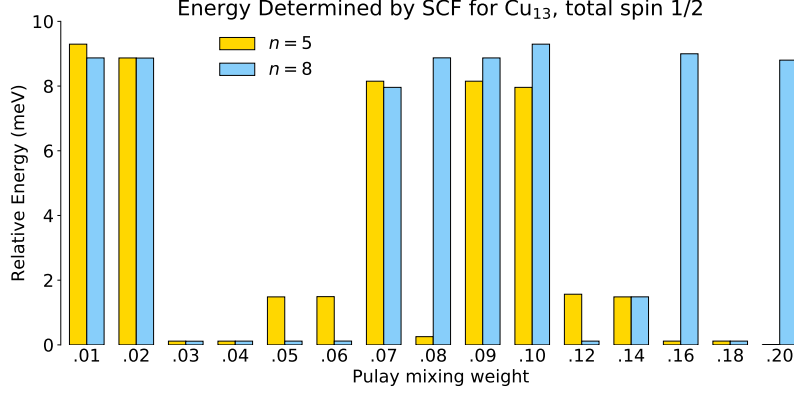


FIG. 3: For a Cu_{13} cluster with fixed total spin $1/2$, we used SCF with Pulay mixing to seek self-consistent Kohn-Sham states. The Pulay mixing configurations are specified by the number n of previous densities used and mixing weight, and the height of the bars indicate the electronic energy of the resulting converged state relative to the lowest energy state obtained with imaginary-time propagation. Notice the variability in the converged state depending on the Pulay parameters, and that 12 of the 30 runs converged to one of the five lowest energy states. The energies here appear in Figure 2 as dashed lines for comparison with the converged states obtained with it-TDDFT, and additional information can be found in Table II.

can be found in Table II. SCF has trouble finding the minimum energy states in this fixed-spin system, likely due to the fact that there are five degenerate states. Figure 2 shows the energy trajectories in imaginary time of 12 different random starting configurations, and each of these converges to one of five lowest-energy states. To help identify the equality of final states, for both the it-TDDFT and SCF runs, we also computed the density distances between each combination of obtained states. States with energies within 10^{-2} meV and a density distance of less than $1/100$ th of an electron of each other were considered equal. The five-fold degeneracy of the lowest energy states in the $m = 1\mu_B$ magnetization of this system is suggested by the calculations in Ref. 28, where it was found that the ground state of the system, with magnetization $m = 5\mu_B$, contains five degenerate valence electrons which have unpaired spins. To obtain a magnetization of $m = 1\mu_B$, four of the electrons would need to pair spins, leaving five possibilities of which electron to leave unpaired. Figure 2 shows the magnetization density, the spin up electron density minus the spin down electron density, of one of these five lowest-energy states. Notice that there are five equivalent ways to place such a magnetization density on the icosahedral shape of the copper cluster, explaining the degeneracy. The visible differences of up to 0.1 meV in the energies of these degenerate states is due to the discretization effects of the real space grid slightly breaking the icosahedral

symmetry.

Our results are better at finding the lowest-energy states compared to SCF, which for different mixing parameters often converges to some other excited states of spin $+1/2$ (the energies of which are shown as dashed lines in the figure). This suggests that it-TDDFT is better for ensuring that the lowest energy state is obtained, instead of using SCF and potentially converging to a low-lying excited state.

In Figure 3, we show the electronic energies of the states obtained using SCF with Pulay mixing, for various mixing parameter choices. In the plot, we see that even small changes in the mixing parameters can result in arriving at a different final state. This can happen in metallic systems where the gap between occupied and unoccupied states is small, since in these systems SCF has a higher chance of converging to an excited state, also a valid self-consistent solution to the KS equations. This is not necessarily a significant drawback, since these same excited states will have energies that are quite close to the ground state energy. Depending on what is desired from the calculation however, the consistency with which it-TDDFT finds the lowest energy states could be of use. For example, in this case it-TDDFT correctly identifies the five-fold degeneracy of the lowest-energy states of $m = 1\mu_B$ copper-13, while some of the SCF runs produce excited states which would not reveal this.

D. Ruthenium Nanocluster Ground State

A 55-atom ruthenium nanocluster was considered by Montemore et al. in Ref. 29, where in computing the ground state, the authors informed us that the spin-unpolarized calculation was difficult to converge with SCF. These discussions motivated us to test our method on this system.

When using Pulay mixing, or other popular schemes like linear mixing, one generally does not worry about setting specific mixing parameters like the number of past densities to mix, or the mixing weight. For example, the default SIESTA²⁵ mixing weight value of 0.25 will result in convergence for many systems. However, if the calculation does not manage to find a self-consistent solution, one way to proceed is to experiment with different mixing parameters until the calculation does complete. This can be a time-consuming and tedious process when working on a computing cluster, where submitted jobs might continue to come back without useful results, consuming processing time while giving little impression

of progress.

In Table I, we show the results of using SCF with Pulay mixing to find the ground state of the spin-unpolarized Ru₅₅ cluster. The number of past densities to mix was kept at $n = 5$ for all trials and mixing weights ranging from 0.02 to 0.20 were tested. Furthermore, we used Fermi electronic smearing for half the trials with $T = 300$ K. The electronic smearing helps with convergence since it allows for fractional occupations near the Fermi level, mitigating charge sloshing effects during the SCF loop. For each run, the table lists the energy of the final step, the density difference $\Delta\rho_{\text{max}}$, and whether the run converged. The energy of the final state is measured relative to the ground state energy calculated with it-TDDFT. The density difference $\Delta\rho_{\text{max}}$ refers to the maximum elementwise difference in the density matrix between the final and penultimate step. This is the quantity used in SIESTA to determine convergence. The convergence criteria we used was $\Delta\rho_{\text{max}} < 10^{-6}$ (SIESTA default is 10^{-4}).

The table shows that only a few mixing weights result in convergence, namely the smallest ones with $T = 300$ K of smearing. In these runs, notice the entropic energy contribution of about 78 meV relative to the ground state energy obtained with it-TDDFT. None of the runs without electronic smearing converge, despite some parameter configurations obtaining energies similar to the ground state energy determined with it-TDDFT. The states resulting from unconverged runs generally should not be trusted as they may not be acceptable approximations to actual solutions, which have to satisfy the KS equations self-consistently. While it may be tempting to use the magnitude of a measure of the density difference from step to step, e.g. $\Delta\rho_{\text{max}}$, as a gauge of how close the present electronic state is to a self-consistent solution, this can only be done when the density difference is clearly heading towards zero. If the SCF loop becomes unproductive, unable to decrease the density difference, there is no guarantee of the quality of the present trial state. For example, in Table I, examining the row with mixing weight 0.10 and comparing the $T = 0$ K and $T = 300$ K cases, we find that even though $\Delta\rho_{\text{max}} = 0.589$ in the latter run is smaller than $\Delta\rho_{\text{max}} = 0.702$ in the former, the energy of the state obtained with $T = 300$ K is more than 6 eV off from the correct ground state energy while the $T = 0$ K run is only about 0.006 eV off. It is important to remember that even if an unconverged run results in an energy that is close to a known ground state energy, other observables calculated with the state may not be accurate since the density used by \hat{H}_{KS} does not correspond to the wavefunction, invalidating the application of DFT.

SCF with Pulay Mixing for Ru ₅₅ , Spin Unpolarized						
$T = 0\text{ K}$				$T = 300\text{ K}$		
Mixing Weight	Energy (meV)	$\Delta\rho_{\text{max}}$	Converged	Energy(meV)	$\Delta\rho_{\text{max}}$	Converged
0.02	-0.012	0.086	No	78.388	9.98×10^{-7}	Yes
0.04	-0.004	0.052	No	78.380	9.83×10^{-7}	Yes
0.06	0.069	0.227	No	78.448	5.31×10^{-7}	Yes
0.08	0.395	0.185	No	78.408	9.01×10^{-7}	Yes
0.10	5.538	0.702	No	6384.947	0.589	No
0.12	73.276	0.730	No	71540.022	0.699	No
0.14	148.995	1.388	No	146157.633	1.391	No
0.16	6.385	0.589	No	235202.686	1.409	No
0.18	295.051	1.441	No	294667.870	1.446	No
0.20	353.573	1.444	No	353794.415	1.455	No

TABLE I: For a spin unpolarized Ru₅₅ nanocluster, we sought to find the ground state electronic configurations using SCF with Pulay mixing, with a $n = 5$ density history length and mixing weights ranging from 0.02 to 0.2. The table shows the electronic energy of the last step, relative to the energy of a converged state determined with it-TDDFT (trajectory shown in Figure 4), calculated with both 0 K and 300 K of Fermi electronic smearing. If SCF found a self-consistent state, the energy reported is physically meaningful, while if it did not, it merely gives an indication of how reasonable the last state is. The columns labeled $\Delta\rho_{\text{max}}$ show the maximum elementwise difference in the density matrix between the final and penultimate step. The convergence criteria we used was $\Delta\rho_{\text{max}} < 10^{-6}$ (SIESTA default is 10^{-4}). Notice that for small mixing weights at 0 K the relative energy suggests that SCF was close to finding the ground state, but the values of $\Delta\rho_{\text{max}}$, which were nondecreasing when the calculation timed out, allude to charge sloshing, impeding convergence.

Applying our it-TDDFT method to the ruthenium system produces the ground state without issue, as illustrated in Figure 4. The observed monotonically decreasing energy and density distance $D[n, n_0]$ show consistent progress, as we expect from the theory. When contrasting this situation to the possibility of stagnation without usable results in the SCF approach, the practical appeal of it-TDDFT is clear. As discussed in Section III E, the dependable improvement of the approximation to the ground state as more computational time is provided, as well as the ability to perform preliminary observables calculations before complete convergence, would be beneficial to researchers studying systems that are difficult to converge.

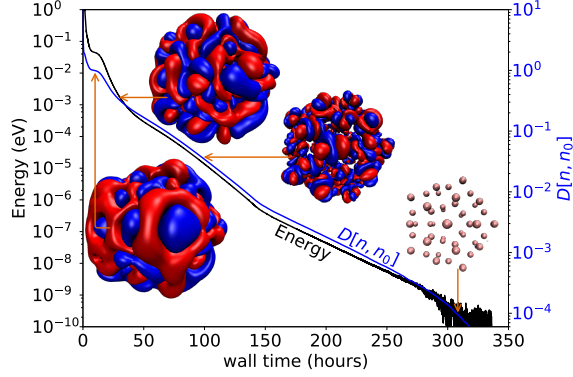


FIG. 4: Electronic energy and density distance ($D[n, n_0]$) trajectory of a spin unpolarized ruthenium cluster (Ru_{55}) measured relative to the state it converges to. The x -axis shows wall time, the time taken to compute on 16 cores of an Intel Xeon Gold 6140. Fixed positive and negative isosurfaces of the density difference $n(\mathbf{r}) - n_0(\mathbf{r})$ are shown at various points in the propagation. SCF with Pulay mixing has trouble finding the ground state of this system, as shown in Table I.

V. CONCLUSION

The first step of any Kohn-Sham DFT calculation is the determination of a self-consistent solution to the KS equations, resulting in a density corresponding to a stationary state of the many-body interacting system. While the standard method of using the iterative SCF loop generally produces a solution, there are important classes of systems that pose problems for this approach due to their small band gaps or degenerate single-particle energies. We have proposed the it-TDDFT method as an alternative means of solving the KS equations in these difficult systems, and shown how it completely avoids the issues which affect SCF.

As we established, the van Leeuwen theorem can be extended to imaginary time, providing a theoretical basis for the expectation of convergence to a stationary state, independent of the exchange-correlation potential and level of theory used in the model system. In addition, we discussed how it-TDDFT could be used in an alternative but equivalent definition for what it means to have found a stationary state in DFT, better suited for metallic systems and systems with degenerate or nearly-degenerate states and based on the time-dependent Kohn-Sham equations. The it-TDDFT method also exhibits numerous practical advantages, such as providing the possibility to calculate approximations to observables of interest before the ground state calculation is fully converged, requiring very few input parameters while achieving robust convergence, and being tolerant to interruptions in the calculation.

In the copper and ruthenium nanoclusters considered in this paper, we demonstrated how

SCF can struggle to find the electronic ground state, either converging to low-lying excited states or getting stuck in charge-sloshing cycles, unable to reduce the density difference from step to step. These systems were readily converged by it-TDDFT, showcasing its robustness through smooth trajectories with monotonically decreasing energy. In the systems discussed in this paper, we either ran the calculation as spin-unpolarized, or with a fixed total spin. This is not an inherent limitation of the method, as one could simply run the calculation with all possible spin polarizations and select the state with the lowest energy. It should also be possible to adapt the method to non-collinear spin systems, since the operating principle depends only on the Hamiltonian being able to differentiate states by energy. Furthermore, while we used finite systems for our example calculations, our method can be extended to find ground states of periodic systems by simultaneously propagating Kohn-Sham states at multiple k -points.

We found that when using it-TDDFT for finding ground states, it is generally between 10 to 100 times slower than using SCF on the same system when the latter converges. However, given that our implementation was primarily for prototyping the method, there are areas that can be improved, whether through more efficient numerical techniques or possible computational shortcuts like extrapolating state trajectories. Despite the higher expected computational cost of it-TDDFT, it is expected to reliably manage the most troublesome systems for SCF, where equally sizable runtimes may be exhausted without achieving convergence.

Given an existing TDDFT code which evolves systems in real-time, it should be relatively straightforward to implement a prototype of the presented it-TDDFT approach, requiring only an imaginary time substitution in the propagation step and a method to orthonormalize the single-particle states. While more efficient implementations could be examined in the future, the low barrier to utilizing it-TDDFT could make it an attractive alternative option for those dealing with particularly vexing systems. Our proposed method should prove to be a useful tool in practical applications of density functional theory.

¹ P. Hohenberg and W. Kohn, Phys. Rev. **136**, B864 (1964), URL <https://link.aps.org/doi/10.1103/PhysRev.136.B864>.

- ² W. Kohn and L. J. Sham, Phys. Rev. **140**, A1133 (1965), URL <https://link.aps.org/doi/10.1103/PhysRev.140.A1133>.
- ³ D. M. Ceperley and B. J. Alder, Physical Review Letters **45**, 566 (1980).
- ⁴ J. P. Perdew, K. Burke, and M. Ernzerhof, Physical review letters **77**, 3865 (1996).
- ⁵ I. Štich, R. Car, M. Parrinello, and S. Baroni, Physical Review B **39**, 4997 (1989).
- ⁶ T. V. Voorhis and M. Head-Gordon, Molecular Physics **100**, 1713 (2002), <https://doi.org/10.1080/00268970110103642>, URL <https://doi.org/10.1080/00268970110103642>.
- ⁷ V. Weber, J. VandeVondele, J. Hutter, and A. M. N. Niklasson, The Journal of Chemical Physics **128**, 084113 (2008), <https://doi.org/10.1063/1.2841077>, URL <https://doi.org/10.1063/1.2841077>.
- ⁸ P. Pulay, Chemical Physics Letters **73**, 393 (1980), ISSN 0009-2614, URL <http://www.sciencedirect.com/science/article/pii/0009261480803964>.
- ⁹ P. Pulay, Journal of Computational Chemistry **3**, 556 (1982), <https://onlinelibrary.wiley.com/doi/pdf/10.1002/jcc.540030413>, URL <https://onlinelibrary.wiley.com/doi/abs/10.1002/jcc.540030413>.
- ¹⁰ M. C. Michelini, R. Pis Diez, and A. H. Jubert, International Journal of Quantum Chemistry **70**, 693 (1998).
- ¹¹ A. D. Rabuck and G. E. Scuseria, The Journal of Chemical Physics **110**, 695 (1999), <https://doi.org/10.1063/1.478177>, URL <https://doi.org/10.1063/1.478177>.
- ¹² N. D. Mermin, Phys. Rev. **137**, A1441 (1965), URL <https://link.aps.org/doi/10.1103/PhysRev.137.A1441>.
- ¹³ M. Verstraete and X. Gonze, Phys. Rev. B **65**, 035111 (2001), URL <https://link.aps.org/doi/10.1103/PhysRevB.65.035111>.
- ¹⁴ P.-M. Anglade and X. Gonze, Phys. Rev. B **78**, 045126 (2008), URL <https://link.aps.org/doi/10.1103/PhysRevB.78.045126>.
- ¹⁵ G. Kresse and J. Furthmüller, Phys. Rev. B **54**, 11169 (1996), URL <https://link.aps.org/doi/10.1103/PhysRevB.54.11169>.
- ¹⁶ V. Peuckert, Journal of Physics C: Solid State Physics **11**, 4945 (1978), URL <http://stacks.iop.org/0022-3719/11/i=24/a=023>.
- ¹⁷ E. Runge and E. K. U. Gross, Physical Review Letters **52**, 997 (1984).

- ¹⁸ R. van Leeuwen, International Journal of Modern Physics B **15**, 1969 (2001).
- ¹⁹ G. Kolesov, E. Kaxiras, and E. Manousakis, Phys. Rev. B **98**, 195112 (2018), URL <https://link.aps.org/doi/10.1103/PhysRevB.98.195112>.
- ²⁰ P. Bader, S. Blanes, and F. Casas, The Journal of Chemical Physics **139**, 124117 (2013), <https://doi.org/10.1063/1.4821126>, URL <https://doi.org/10.1063/1.4821126>.
- ²¹ L. Lehtovaara, J. Toivanen, and J. Eloranta, Journal of Computational Physics **221**, 148 (2007).
- ²² E. R. Hernández, S. Janecek, M. Kaczmariski, and E. Krotscheck, Phys. Rev. B **75**, 075108 (2007), URL <https://link.aps.org/doi/10.1103/PhysRevB.75.075108>.
- ²³ M. Aichinger and E. Krotscheck, Computational Materials Science **34**, 188 (2005), ISSN 0927-0256, URL <http://www.sciencedirect.com/science/article/pii/S0927025605000029>.
- ²⁴ G. Kolesov, O. Grånäs, R. Hoyt, D. Vinichenko, and E. Kaxiras, J. Chem. Theory Comput. **12**, 466 (2016).
- ²⁵ J. M. Soler, E. Artacho, J. D. Gale, A. García, J. Junquera, P. Ordejón, and D. Sánchez-Portal, Journal of Physics: Condensed Matter **14**, 2745 (2002).
- ²⁶ T. Kowalczyk, S. R. Yost, and T. Van Voorhis, The Journal of Chemical Physics **134**, 054128 (2011).
- ²⁷ V. A. Basiuk, International Journal of Quantum Chemistry **111**, 4197 (2011), <https://onlinelibrary.wiley.com/doi/pdf/10.1002/qua.23003>, URL <https://onlinelibrary.wiley.com/doi/abs/10.1002/qua.23003>.
- ²⁸ R. A. Hoyt, M. M. Montemore, and E. Kaxiras, The Journal of Physical Chemistry Letters **9**, 5339 (2018), pMID: 30145896, <https://doi.org/10.1021/acs.jpclett.8b02133>, URL <https://doi.org/10.1021/acs.jpclett.8b02133>.
- ²⁹ M. M. Montemore, R. Hoyt, G. Kolesov, and E. Kaxiras, ACS Catalysis **8**, 10358 (2018), <https://doi.org/10.1021/acscatal.8b03266>, URL <https://doi.org/10.1021/acscatal.8b03266>.

VI. SUPPLEMENTAL MATERIALS

States Determined by SCF with Pulay Mixing for Cu₁₃, total spin 1/2

	Mixing Weight	Energy (meV)	Time (min)	Min. State
$n = 5$				
	0.01	9.2955	2021.7	No
	0.02	8.8690	2386.0	No
	0.03	0.1155	18.7	Yes
	0.04	0.1156	51.0	Yes
	0.05	1.4833	30.7	No
	0.06	1.4910	64.1	No
	0.07	8.1505	163.4	No
	0.08	0.2538	28.0	Yes
	0.09	8.1506	61.2	No
	0.10	7.9600	60.3	No
	0.12	1.5656	22.8	No
	0.14	1.4832	34.3	No
	0.16	0.1163	7.0	Yes
	0.18	0.1170	6.8	Yes
	0.20	0.0003	7.4	Yes
$n = 8$				
	0.01	8.8701	787.8	No
	0.02	8.8656	750.6	No
	0.03	0.1135	26.8	Yes
	0.04	0.1162	14.9	Yes
	0.05	0.1164	15.4	Yes
	0.06	0.1176	13.9	Yes
	0.07	7.9599	29.3	No
	0.08	8.8722	119.4	No
	0.09	8.8698	207.5	No
	0.10	9.2955	137.4	No
	0.12	0.1159	17.9	Yes
	0.14	1.4844	15.3	No
	0.16	8.9980	32.0	No
	0.18	0.1162	10.7	Yes
	0.20	8.8015	54.8	No

TABLE II: For a Cu₁₃ cluster with fixed total spin 1/2 and 0 K of Fermi electronic smearing, we used SCF with Pulay mixing to seek self-consistent Kohn-Sham states. For the Pulay mixing configurations specified by the number n of previous densities used and mixing weight, the table shows the electronic energy of the converged state relative to the lowest energy state obtained with it-TDDFT, the wall time taken to reach convergence, and whether the converged state matches one of the five lowest-energy states determined with it-TDDFT. The energies in this table can be compared to the it-TDDFT energy trajectories shown in Figure 2 where they appear as dashed lines. The wall times in this table can also be compared to the wall time plotted in Figure 2 since the calculations were given identical resources.